archaeometry

Archaeometry **59**, 3 (2017) 511–527 doi: 10.1111/arcm.12260

A ROCK-MAGNETIC QUEST FOR POSSIBLE ORE SOURCES FOR THE ANCIENT IRON-SMELTING INDUSTRY IN THE OLKHON REGION (LAKE BAIKAL, SIBERIA)*

G. G. MATASOVA†

Trofimuk Institute of Petroleum Geology and Geophysics SB RAS, Novosibirsk, Russia

A. YU. KAZANSKY

Geological Faculty of Lomonosov Moscow State University, Moscow, Russia and Institute of Archaeology and Ethnography SB RAS, Novosibirsk, Russia

N. O. KOZHEVNIKOV

Trofimuk Institute of Petroleum Geology and Geophysics SB RAS, Novosibirsk, Russia

S. V. SNPOKOV

Irkutsk State University, Irkutsk, Russia

and A. V. KHARINSKY

National Research Irkutsk State Technical University, Irkutsk, Russia

Rock-magnetic techniques were used to examine the topsoil layer of Kurma archaeological site (in the Olkhon region, on the north-western coast of Lake Baikal, Siberia) in an effort to determine the possible sources of iron ores for iron-smelting centres (at about the BC/AD *boundary). Measurements have shown a magnetic enhancement of the topsoil due to magnetite grains resulting from weathering of strongly magnetic crystalline rocks. They have also revealed a preliminary picture of the distribution of strongly magnetic topsoils around the ancient iron-smelting centres. Perhaps, in addition to traditional sources of raw materials, the ancient metallurgists used black sand talus as an ore deposit.*

KEYWORDS: ANCIENT IRON SMELTING, ROCK-MAGNETIC STUDY, TOPSOIL, MAGNETITE, KURMA ARCHAEOLOGICAL SITE, BAIKAL, SIBERIA

INTRODUCTION

Recently, the rock-magnetic method has increasingly been used as a powerful tool in various applications of Quaternary geology, such as sediment source tracing, palaeoenvironmental and climate reconstruction, and anthropogenic pollution (Evans and Heller 2003). Although this method has been used at some archaeological sites (see, e.g., Batt *et al.* 1995; Ellwood *et al.* 1997; Dalan and Banerjee 1998; Morinaga *et al.* 1999; Gose 2000; Peters *et al.* 2001; Evans and Heller 2003; Herries 2009), its use has been rather sporadic, and its potential as a new archaeological tool is still underestimated. In this study, we have applied this method to determine a

*Received 2 July 2015; accepted 11 April 2016
†Corresponding author: email matasovagg@ipgg.sbras.ru

potential source of raw material for the ancient iron-smelting industry on the north-western coast of Lake Baikal.

The end of the first millennium BC in the Baikal region was characterized by the prevalence of iron products. Most of them probably had been manufactured locally, as evidenced by the remains of the iron-smelting industry, recorded in different parts of the region (Agafonov and Kozhevnikov 1999; Kozhevnikov *et al.* 2001; Kharinsky and Snopkov 2004). One of the areas where several bloomeries for iron smelting operated continuously for a long time was located on the west bank of the Small Sea Strait of Lake Baikal, south-west of the Kurma river (Fig. 1). To date, due to the results of magnetic prospecting, three metallurgical centres have been discovered there—'Kurma Lake 1', 'Kurma 28' and 'Kurma 18'. Excavation of two of them ('Kurma Lake 1' and 'Kurma 28') (Kharinsky and Snopkov 2004) has revealed the remains of bloomeries, slag pits and connecting channels, as well as the remains of burnt charcoal and a large number of slag blocks. However, it is still the case that no visible traces of ore have been found. Only at 'Kurma Lake 1' we have recognized some fragments of magnetite, but whether they were used for iron production is still unclear. The absence of iron ore residues and ore grinding evidence poses questions about the type of raw materials used and their possible sources.

The Olkhon region does not belong to areas with industrial iron ore deposits, but iron production in antiquity required much less raw material than at the present time. Therefore, the ancient people could use poor (in the modern sense) local occurrences, such as limonite and hematite concretions, which are widespread in the Olkhon region (Kozhevnikov *et al.* 2001). However, the resources of such ores were not sufficient for the stable operation of iron-smelting centres, so the question of ore sources for ancient iron metallurgy remains open. In order to find a possible source of raw material for the ancient metallurgists in the Olkhon region, in 2011–13 we performed a rock-magnetic study of the Kurma site topsoil. The decision to use rock-magnetic methods was determined by general considerations about a possible link between the ancient metallurgical activity and topsoil magnetism in the vicinity of smelting sites (Birch *et al.* 2015). It is well known that, due to human industrial activity, the magnetic properties of soil and/or sediment may undergo certain changes (Evans and Heller 2003). At archaeological sites, the most dramatic changes are observed in the territory of ancient metallurgical complexes (Vernon *et al.* 1998; Powell *et al.* 2002). Here, under the influence of high temperatures, the magnetic susceptibility of upper soil layers increases due to the neoformation of magnetic minerals (magnetite) as a result of the baking of soil organic matter. This allows us to find and to map areas that in ancient times were exposed to high temperatures during iron smelting: slag heaps, baked zones, and zones of preparation of raw materials and of charcoal production. A large amount of research has been published in which the results of the use of rock-magnetic methods for solving various problems of archaeology have been presented and discussed. In centres of ancient metallurgy in the United Kingdom (Powell *et al.* 2002) and Denmark (Abrahamsen *et al.* 2003), this method has proven to be a reliable way of obtaining detailed information, complementing traditional archaeological research. The high performance of magnetic methods arises from the fact that the remains of bloomeries, large slag blocks and baked sediments are characterized not only by high magnetic susceptibility but also by high thermoremanent magnetization, which provides high magnetic anomalies over these objects. Large clusters of slag fragments can also be marked by magnetic field anomalies generated by the induced magnetization (Kozhevnikov *et al.* 1998). In addition to rock-magnetic methods, the archaeomagnetic study of large monolithic slag blocks is used to determine the age of individual sites or groups of sites (Abrahamsen *et al.* 2003; Peters *et al.* 2008). Furthermore, rock-magnetic study of slag can be used to recover characteristics of the iron-working process—for example, the oxidizing

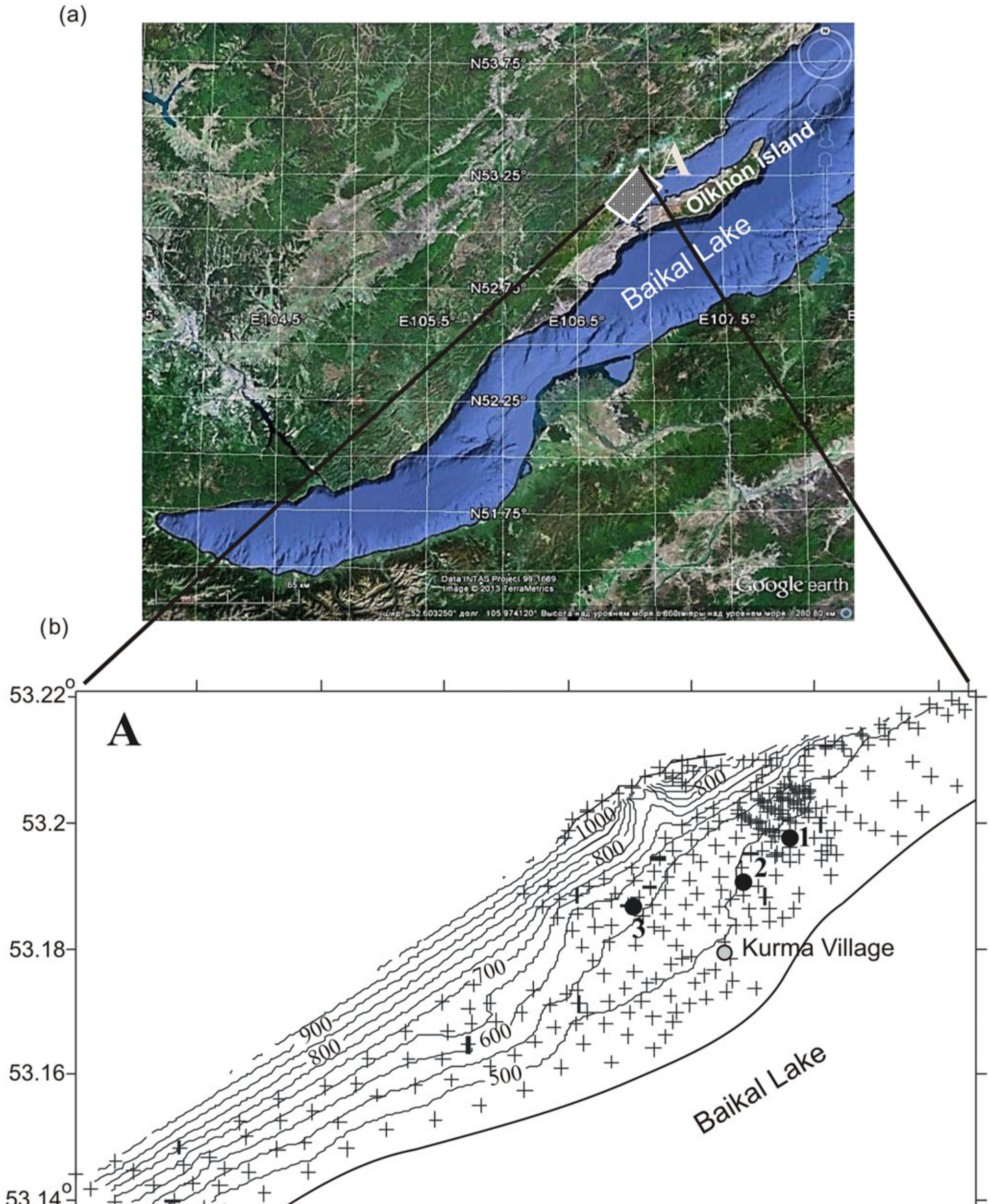

Figure 1 *The location of the study area: (a) a Google Earth space image of the eastern part of the Baikal region; (b) a sketch map of the Kurma archaeological region, with altitude contour lines at intervals of 50 m. The crosses mark the points of in situ magnetic susceptibility measurement and sampling. The black circles show the iron-smelting centres: 1, 'Kurma Lake 1'; 2, 'Kurma 28'; 3, 'Kurma 18'. [Colour figure can be viewed at wileyonlinelibrary.com]*

and/or reducing conditions inside the bloomery and its inner temperature, the efficiency of iron extraction from the ore and ore source identification—and to determine whether the slag has solidified inside or outside the bloomery (Peters *et al.* 2008).

The above concise review shows that in the case of archaeometallurgical research, the rock-magnetic method is used to study mainly slags and fragments of iron-smelting kilns, and not the surrounding sediments. The few exceptions are: a paper by Vigliotti *et al*. (2003), where the magnetic properties of marine sediments deposited during the past 4000 years in the Corsican Strait are discussed in connection with the reconstruction of the ancient iron-smelting industry on the island of Elba; and another paper, by Mighall *et al.* (2009), describing the study of magnetism of fine particles that were formed during the bloomery process and that accumulated in the peat of a nearby bog. Environmental pollution by metallurgical wastes from the ancient smelting sites has been also discovered in the bottom sediments of Lake Lozhka in western Siberia by the authors of this paper (Kazansky *et al.* 2007). However, such studies are at an early stage as yet, so any experience with regard to the magnetic investigation of topsoil at smelting sites, possible iron ore sources and slags for solving the above problems is of great interest (Peters *et al.* 2008).

THE GEOLOGICAL SETTING

In geological terms, the Olkhon region belongs to the folded frame of the Siberian platform. The western coast of Lake Baikal, in the Small Sea Strait, is composed of highly metamorphosed rocks of the Olkhon group. Traditionally, the age of the group is estimated as Archean to Early Proterozoic (Kochnev 2007).

The Olkhon group contains crystalline schist of amphibole, pyroxene–amphibole and biotite–amphibole composition, biotite, garnet–biotite and pyroxene–amphibole gneiss; calcite and dolomite marble; and quartzite. All rocks are characterized by high-temperature metamorphism of granulite and amphibolite facies and widely developed migmatization. The geological history of the Olkhon crystalline complex appears to be a multistage metamorphic evolution, closely related to deformation and magmatic processes in the region. Such an evolution, in turn, determines the complexity of the structure of the ancient strata. For decades, the geology of the Olkhon region has been subject to discussion. A commonly accepted scheme for the stratigraphy, tectonics, metamorphism and magmatism of this area still does not exist (Ryazanov 1993; Kochnev 2007; Shulga 2010).

The Cenozoic sediments of the Olkhon region are directly related to the development of the Lake Baikal basin. Most of the sediments are of coastal-lake, alluvial–proluvial and proluvial–slope wash genesis. The Pleistocene–Holocene complex is represented by a series of river and lake terraces (Ryazanov 1993).

The tectonic position of the Olkhon region is determined by its belonging to the Baikal Rift Zone, as well as its proximity to the marginal suture edge seam of the Siberian Platform and the Baikal mountain-folded region. Faulting is associated with movements of the platform along the marginal suture and the development of the Baikal Rift zone. The largest fault in the area, the Primorsky fault, is connected with the marginal suture system of the Siberian platform. The tectonic zonation of the Baikal region suggests three geomorphological areas—the Primorsky mountain ridge, the Near-Olkhon Plateau and the Lake Baikal depression—separated by regional deep faults (Primorsky and Near-Olkhon) (Kochnev 2007). The Near-Olkhon plateau is a fault scarp of the Primorsky fault, separating the rift valley from the Primorsky Range.

A series of weakly expressed depressions are observed on the fault scarp surface, which is gradually transforming into a flattened inclined surface at the base of the slope. These depressions present solifluction valleys. The material involved in solifluction flow forms dome-shaped structures at the foot of the slope. The Primorsky fault is complicated by numerous intermediate tectonic steps. These steps on the slope of the Primorsky Range are well pronounced in the area near the Sarma and Kurma rivers, and are represented by small blocks on the bottom side of the Baikal Rift (Ufimtsev 1995). A more detailed description of the geology and tectonics of the Olkhon region is given in Snpokov *et al.* (2012).

POSSIBLE SOURCES OF IRON ORE IN THE OLKHON REGION

There are several types of iron ore deposit within the territory of the Olkhon region, including the west coast of the Maloe More Strait, near the mouths of the Sarma and Kurma rivers. According to the local minerogenic subdivision, this district belongs to the Tazheran metallogenic zone, in which different magmatogenic, metamorphogenic and polygenic mineral deposits, including iron ores, are widespread (Kochnev 2007; Shulga 2010).

Magmatogenic iron ore

Such occurrences are represented by magnetite from aplite granite, granite–pegmatite and quartz veins. These veins are of small thickness and include mainly disseminated nested clusters of magnetite. Because of the low concentrations, it is unlikely that the magnetite from pegmatite veins was used by the ancient metallurgists.

Metamorphic iron ore

These occurrences include amphibolite, gneiss and crystalline schist with a high concentration of magnetite and micro-layered ferruginous quartzite. Magnetite ores of these occurrences are connected with sericite–chlorite schist, where they form a series of layers. The ore is banded; the banding is caused by alternating layers of quartzite and layers of massive magnetite. The iron content of magnetite in quartzite varies from 20% to 48%. Fragments of magnetite quartzite were found during excavation of the ‘Kurma Lake 1’ metallurgical centre (Kharinsky and Snopkov 2004). A significant obstacle to use of the quartzite as iron ore is its high hardness, which complicates crushing in preparation for metallurgical processes.

Brown iron ore of weathering crust

This type belongs to the polygenic iron ore deposits. Such ores are widely developed in the Olkhon region. Most often, they make up a horizontal ore-body, elongated in the direction of the bedrock strike. These deposits may represent placers of ironstone pebbles consisting either of a massive brown ore or breccia-like formations, in which small rounded quartz grains are cemented by massive ironstone.

Certain volume ratios between ‘hard’ and ‘loose’ components of the ore-body are observed in brown iron ore deposits, which fluctuate in the range from 1:1 to 1:6. Brown iron ores are represented by limonite, hematite and martite. The iron content in ores ranges from 11.7% to 61.1% (Fe_2O_3 80%); some ores also contain up to 3.9% of manganese oxide. The dimensions of the ore deposits reach up to 150–250 m in length and 60 m in width. The thickness of the deposits varies from several centimetres to several metres. Due to their easy access and high iron content, deposits of bog iron ore and ore pebble placers were probably one of the sources of raw material for iron production in antiquity.

Deluvium (talus) deposits with placer magnetite

Field measurements of the magnetic susceptibility of the topsoil at the foot and on the slopes of the Primorsky Range showed that the concentration of magnetic material in the soil is extremely heterogeneous. The magnetic susceptibility of the soil varies 200-fold. The source of the magnetic material is more likely to be magnetite gneiss, crystalline schist and ferruginous quartzite. These rocks, being destroyed by physical weathering, provide abundant magnetic material. Under the action of gravitational sliding and slopewash, the material is moved down slope and is deposited at its base, where the water flow velocity decreases dramatically. Moreover, this heavier and more hydroscopic material (sand, debris) is deposited faster than one that is lighter and less permeable (clay, silt). Therefore, due to its high density, the black sand is deposited in a narrow band in the transition zone between the slope of the Primorsky Range and its piedmont plain. Further down, at the flattening slope of the foothill plains, the concentration of magnetic material in the soil is reduced. Perhaps the ancient metallurgists could have used magnetite ore from the foothill talus deposits. Black magnetite sand is a source of ore, which requires no complex pre-processing. The separation of magnetite sand could have been carried out by washing. During the excavation, we did not find any devices for crushing and abrasion of ores. Therefore, we have identified two types of iron ore as a possible source of raw material, which do not require complex preparation for metallurgical processes: (1) brown iron ore pebbles from weathering crust and (2) the black sand of talus deposits. The high iron content in ores causes their high magnetism, so we used the rock-magnetic method in order to reveal a distribution of iron ores over the study area.

METHODS AND DATA

Field measurements and sampling

Field measurements of the magnetic susceptibility of the ground surface were performed over an area of ~30 km^2 around the village of Kurma. The area is located between 53.1352°N and 53.221°N and 106.8606°E and 107.061°E (Figs 1 (b) and 1 (c)). Measurements of the magnetic susceptibility (K) were carried out using a KT-5 (AGICO, Czech Republic) field susceptibility meter on the levelled ground surface after removal of sods (3–5 cm). The study areas were located in various geomorphological conditions—mountains, rocky places, sometimes densely afforested areas with large differences in altitude, steep slopes and mountain river valleys—so the distance between measurement points was chosen depending on real opportunities, and ranged from 200 to 500 m (Fig. 1 (c)). In total, 320 field measurements were made. The magnetic susceptibility measurements of the topsoil were conducted with several objectives:

(1) to identify the ‘background’ (typical for the area and the type of soil) magnetic susceptibility values;
(2) to determine whether there are magnetic susceptibility anomalies on the study site and their possible sources; and
(3) to reveal the predominant trends in the distribution of magnetic material and the possible mechanism of its transport over the study area.

In addition to the field measurements at each site, we collected rock-magnetic samples for laboratory experiments (a total of 320 samples). We also measured the magnetic susceptibility of bedrock fragments (if any), scattered on the ground surface within 5 m around the measured site (147 measurements). We found it necessary to measure the magnetic susceptibility of bedrock in the outcrops, which were found at altitudes of 900 m or more (80 measurements). Typical samples of all kinds of rocks were taken for laboratory tests (35 samples).

Laboratory treatment

The low- and high-frequency volume magnetic susceptibilities (K_{LF} and K_{HF} respectively) were measured on the Bartington MS2 susceptibility bridge using a dual frequency probe. For this measurement, the soil samples were placed in standard plastic boxes $2 \times 2 \times 2$ cm in size.

The frequency-dependent magnetic susceptibility (Δ_{FD}) is an absolute difference between two measurements, $\Delta_{FD} = K_{LF} - K_{HF}$, and *FD* (%) is a percentage ratio: $\Delta_{FD}/K_{LF} \times 100\%$.

Hysteresis characteristics were obtained on the J-Meter coercive spectrometer (Jassonov *et al.* 1998). Induced magnetizations such as the saturation magnetization (J_i), the saturation isothermal remanent magnetization (J_r) and the magnetization of the paramagnetic fraction (J_{par}) were acquired by exposure to a magnetic field of 700 mT. The coercive force (B_c) and the remanent coercive force (B_{cr}) were calculated from the hysteresis loops.

The mass-normalized magnetic susceptibility of the paramagnetic and ferromagnetic fractions (K_p and K_{fer}, respectively) and their sum—the initial magnetic susceptibility—were also calculated from the hysteresis loops. The correction for the paramagnetic contribution was made for B_c and K_{fer}.

The magnetic 'hardness', *S*, is calculated as the ratio of the remanent magnetization in the reversed field of 300 mT to the saturation isothermal remanent magnetization in the field of 700 mT: $S = -J_{r(-300)}/J_r$.

The temperature dependence of induced magnetization, $J_s(T)$, in a field of 650 mT was measured using the thermomagnetic analyser (Curie balance) designed by J. K. Vinogradov (IPE), while the temperature dependence, $K(T)$, was studied using a MFK1-FA Kappabridge (AGICO Inc., Brno, Czech Republic). The maximal temperature of heating in both experiments was 700 °C.

RESULTS

Field magnetic susceptibility measurements

The results of the topsoil magnetic susceptibility (*K*) field measurements are presented as a map in Figure 2 (a). The three different areas are clearly recognizable on the map: high (A), moderate (B) and low (C) values of magnetic susceptibility. In area A, *K* is usually higher than 15×10^{-3} SI units; the average *K* values of area B fall between 3×10^{-3} and 15×10^{-3} SI units; and area C shows low values of *K*, less than 3×10^{-3} SI units. Such low susceptibility values are widespread over the greater part of the territory (~ 70%), they are typical for steppe soils in the south-western part of the area and are accepted as background ($K = 2 \times 10^{-3}$ SI units) values for the whole study area. Similar *K* values are found in forest soils in small valleys and combes all over the area. The lowest values of the magnetic susceptibility ($K < 1.5 \times 10^{-3}$ SI units) are typical for bog and alluvial soils undergoing constant or periodic waterlogging.

The highest values of *K* are typical for the soils on steep mountain slopes and along a narrow strip (about 10% of the area) in the foothills of the north-eastern part of the study area. Here, on the Primorsky Ridge, at altitudes more than 800 m above sea level, we found bedrock expositions of schist, gneiss and ferruginous quartzite with very high values of magnetic susceptibility, more than 100×10^{-3} SI units.

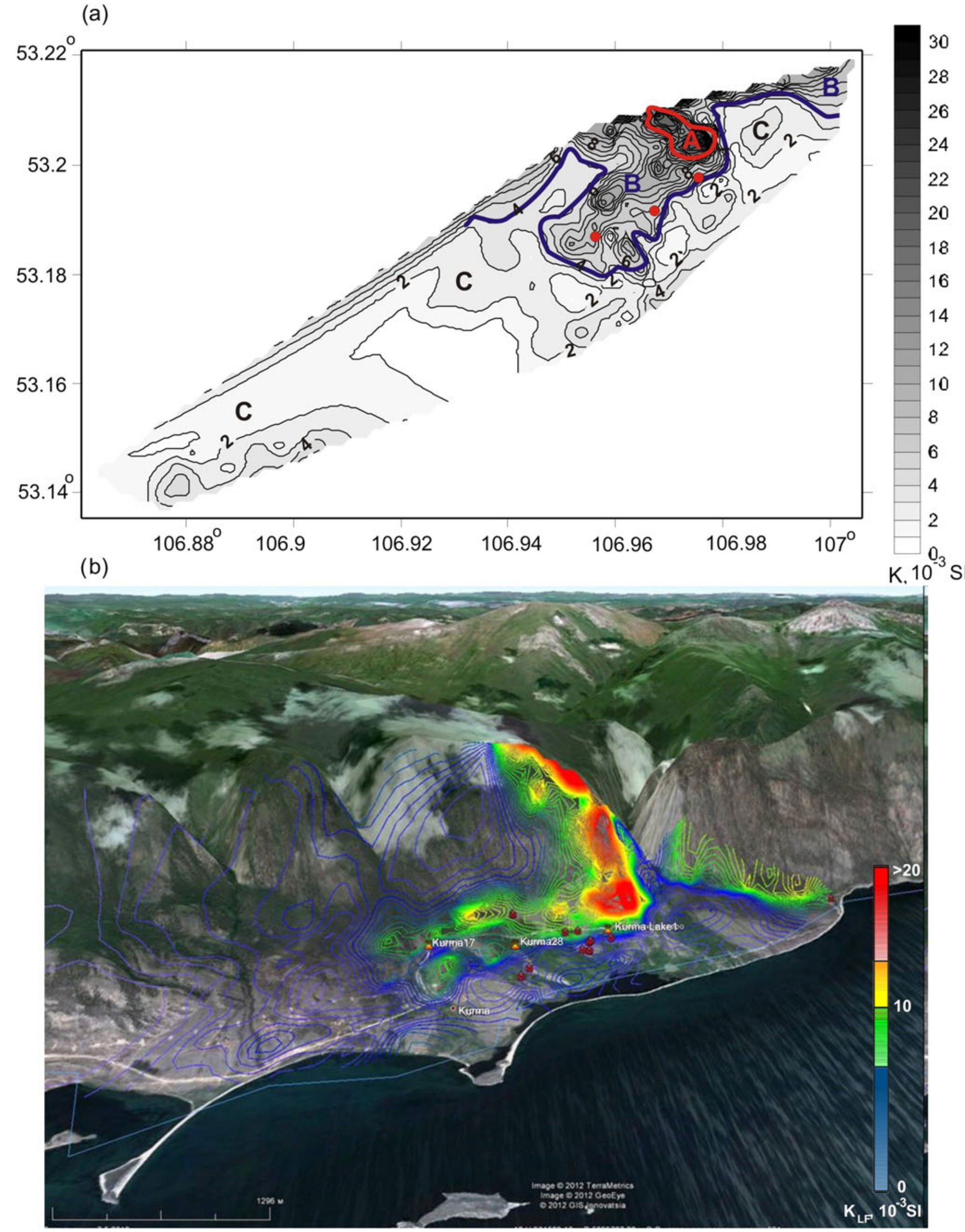

Figure 2 *The distribution of magnetic susceptibility in topsoil over the Kurma archaeological region. (a) A sketch map of the topsoil magnetic susceptibility (field measurements): red circles, ancient iron-smelting centres; areas A, B, and C, see description in the text. (b) A Google Earth space relief image with* K_{lf} *contours (laboratory measurements): orange symbols, ancient iron-smelting centres; red symbols, locations of slag blocks. [Colour figure can be viewed at wileyonlinelibrary.com]*

The moderate K values were found in the steppe soils of the central part of the study area, which cover the watersheds and piedmont plain, gently sloping down to the shore of Lake Baikal.

All iron-smelting centres in Kurma archaeological district, both those already excavated and those assumed on the basis of magnetometer surveys, are located in area B, with moderate values of magnetic susceptibility of the surface soil, but close to the border with area C, which has low values (Fig. 2 (a)).

Laboratory measurements: concentration-sensitive magnetic parameters

Laboratory studies of the concentration-sensitive magnetic parameters of the surface ground confirmed the general picture obtained through the field measurements of the magnetic susceptibility. The distribution pattern of the low-frequency volumetric magnetic susceptibility (K_{LF}) of topsoil measured in the laboratory is shown in Figure 2 (b) contours-on-relief model. It is quite similar to the results of the field measurements (Fig. 2 (b)). The K_{LF} values of the topsoil vary from 20×10^{-5} to 4000×10^{-5} SI units. The highest values of K_{LF} are shown by area A (more than 1500×10^{-5} SI units). Area C is characterized by low values of K_{LF} (less than 200×10^{-5} SI units). The same subdivision into three different areas can also be made on the basis of other rock-magnetic parameters that depend primarily on the concentration of magnetic material.

This thesis is supported by the close correlation between the rock-magnetic parameters. The correlation coefficients (r) between the various parameters range from 0.75 to 0.95 (Figs 3 (a) and 3 (b)). The contribution of paramagnetic minerals (as estimated from parameters K_{par}, J_{par} and their ratios to the ferrimagnetic component) varies from tenths of a per cent (for strongly magnetic soil) up to 20% (for moderately magnetic soil). In weakly magnetic soils, the paramagnetic contribution is more significant (from 5% to 90%) and even exceeds the ferrimagnetic contribution in the two weakest soil samples (Fig. 3 (c)).

Due to its colour, texture, degree of secondary changes and magnetic properties, the bedrock can be divided into three groups: (1) gneiss and granite gneiss; (2) ferruginous quartzite; and (3) brown iron ores.

The rocks of the first two groups are strongly magnetic (Figs 3 (d) and 3 (e)). They are generally exposed in bedrock outcrops, and in the form of debris all over the study area. The magnetic susceptibility of gneiss and granite gneiss varies from 1000×10^{-5} to $10\,000 \times 10^{-5}$ SI units, and these values, on average, coincide with those in the soil, but the maximum K_{LF} values in crystalline rock are about 2.5 times higher than that of most highly magnetic soil near the crystalline outcrops. The gneiss-like granite (granite gneiss) has the lowest values of magnetic susceptibility.

The magnetic susceptibility of ferruginous quartzite varies from 300×10^{-5} to 1500×10^{-5} SI units. The limits of the magnetic susceptibility values for gneiss and quartzite partly overlap. Brown iron ores in landslides of outcrops are generally represented by weathering crust of granite gneiss. These deposits are loose and have a reddish-brown colour, depending on the degree of weathering. They are characterized by relatively low values of magnetic susceptibility (1×10^{-5} to 200×10^{-5} SI units).

All rocks mentioned above also demonstrate strong correlation between their concentration-sensitive magnetic characteristics (the correlation coefficients vary from 0.6 to 0.9). The paramagnetic and antiferromagnetic contributions to the magnetic properties of rocks from the first two groups are similar to those of soils, reaching 20% (Fig. 3 (f)). In brown iron ores, we found samples in which the contribution of paramagnetic and antiferromagnetic materials far exceed that of the ferrimagnetic component. Such interdependence suggests that the magnetic properties

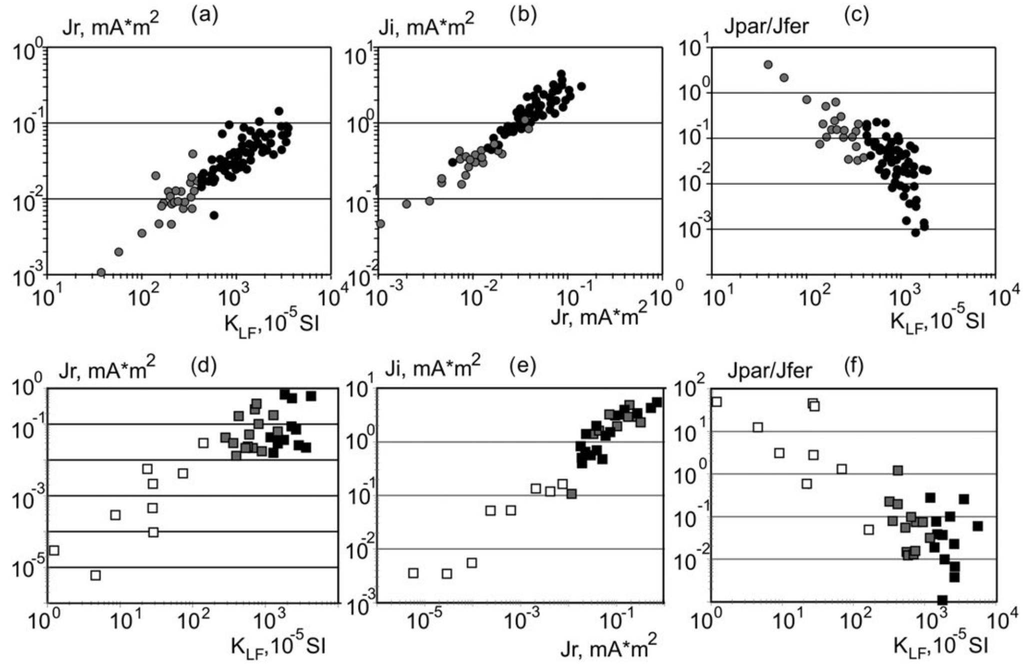

Figure 3 *The correlation between the concentration-sensitive magnetic characteristics of soils (a–c) and bedrock (d–f): grey circles, low-magnetic soil; black circles, the moderately and strongly magnetic soil; white squares, brown iron ore; grey squares, ferruginous quartzite; black squares, gneiss and granite gneiss.*

of the soils and surrounding rocks (except for the low-magnetic soils and brown iron ore) are determined mainly by ferromagnetic minerals. Brown iron ore, in contrast, consists mainly of paramagnetic and antiferromagnetic minerals.

Thermomagnetic analysis of the behaviour of J_s and K in samples during continuous heating up to 700 °C indicates that the vast majority of samples show Curie temperatures of magnetite or Fe-rich titanomagnetite, with the composition very close to that for magnetite (T_c = 540–580 °C) (Fig. 4 (a)). In several samples, mostly in weakly magnetized soils, residual J_s values after heating to over 580 °C retain up to 3–4% of the initial J_s value (before heating). This may indicate the presence of a small quantity of hematite or a high-level paramagnetic background (Fig. 4). In weakly magnetized soils, as shown above (Fig. 3 (c)), such a background can be significant. The ratio $J_{s(2)}/J_{s(1)}$, where the numbers in brackets denote J_s values before and after the first heating, can exceed 1.25–1.30. This means magnetic enhancement of the primary sample after the first heating by newly formed magnetic mineral—that is, magnetite—according to the Curie point of ~575 °C. Magnetite neoformation is most likely to be caused by the reduction of thermal alteration products of Fe-bearing paramagnetic minerals during heating in the presence of organic matter in the sample (Liu *et al.* 2005).

Gneiss, granite gneiss and quartzite contain only magnetite/titanomagnetite with Curie temperatures of 540–580 °C (Figs 4 (d) and 4 (e)). In brown ironstone (Fig. 4 (e)), the J_s values after heating above 600 °C remain constant, which indicates either a high-level paramagnetic background or, possibly, the presence of hematite, although its Curie point is not expressed. In addition, the thermomagnetic curve of the first heating of ironstone demonstrates two distinct bends (at T ~ 130 °C and T = 350 °C), which are not reproduced when reheated. The first inflection

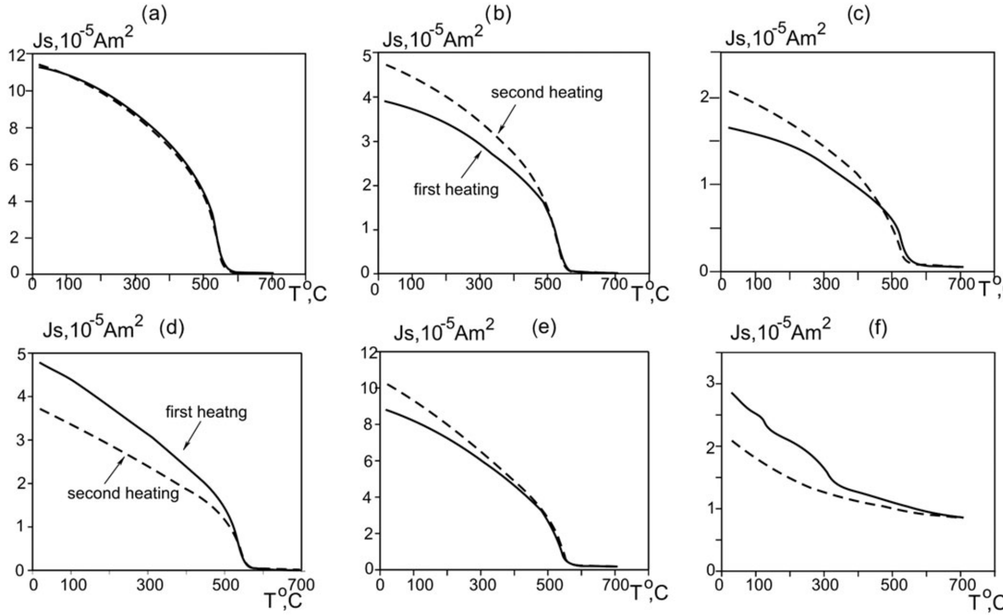

Figure 4 *Typical thermomagnetic curves of J_s for soil and bedrock: (a) strongly magnetic; (b) moderately magnetic; (c) low-magnetic soil; (d) gneiss, quartzite; (e) granite gneiss; (f) ironstone.*

corresponds to the decay of iron hydroxide (goethite) and the second to the transition of maghemite to hematite (Dunlop and Özdemir 1997), which results in a 1.5-fold decrease in J_s. The temperature dependencies shown in Figure 4 demonstrate the conformities of the magnetic fraction of soil and bedrock (gneiss, granite gneiss, quartzite). The main magnetic mineral in soils and in the bedrock is magnetite. In contrast, brown iron ores contain iron hydroxides (goethite), maghemite and possibly hematite.

Laboratory measurements: hysteresis and structure-sensitive properties

The value of the coercive force (B_c) in soil samples varies from 2.5 to 7.2 mT, while the remanent coercive force (B_{cr}) varies from 19 to 42 mT. These ranges are typical for all soil regardless of values of magnetic susceptibility. The low values of both coercive forces indicate a predominance of low-coercive ('magnetically soft') magnetic minerals in the magnetic fraction of soils.

Wider ranges of coercive forces (2.7–13.4 mT for B_c and 16–55 mT for B_{cr}) were found in granite gneiss, quartzite and gneiss. For brown iron ores, the coercivity limits are shifted towards higher values (5.4–9.2 mT for B_c, 30–83.5 mT for B_{cr}). This indicates the presence of a certain amount of high-coercive ('magnetically hard') minerals and/or smaller (as compared to other rocks) grains of magnetic minerals. The 'magnetic hardness" (S-ratios) of strongly magnetic soils do not differ from 1.0, while in the group of moderately magnetic soils this parameter varies from 0.98 to 1.0. In weak samples, its value is reduced to 0.95–0.97. Such changes indicate a slight increase in the contribution of high-coercive minerals to the total magnetism of soils formed on alluvial deposits, compared with soils of mountain slopes and foothills. For the granite gneiss, quartzite and gneiss, $S = 1.0$; for the brown iron ore, S is reduced to 0.45–0.7.

Variations of coercive parameters and *S*-ratio values suggest that the concentration of weakly magnetic soil minerals (such as hematite/goethite) is not high, but in brown iron ores they play a significant role.

Structure-sensitive parameters may help to assess the relative size of magnetic mineral grains. The ratio between two different parameters, approximately equally dependent on the concentration of magnetic minerals, on the one hand, and the sizes of magnetic grains, on the other, makes it possible to obtain quantitative estimations (Thompson and Oldfield 1986). The majority of soil samples contain from 0.1% to slightly over 1% of magnetite (Fig. 5 (a)) and almost the same variations of magnetite concentration (0.1–3.2%) were observed in bedrock (Fig. 5 (b)). The size of magnetic particles in soil is generally above 30 μm, while in bedrock the scatter of magnetic grains is significant, from less than 1 μm to over 100 μm.

For quartzite and gneiss, despite approximately same concentration of the magnetic fraction, the magnetite grain sizes can vary between wide limits (Fig. 5 (b)).

Such a scatter is also indicated by the so-called Day plot of the domain state (DS) of magnetite grains (Day *et al.* 1977), in combination with the theoretical curve of a mixture of single-domain (SD) and multidomain (MD) grains (Dunlop 2002) (Figs 5 (c) and 5 (d)). The magnetic fraction consists almost entirely of MD grains (Fig. 5); the possible portion of SD particles does not exceed 5%.

Magnetic grains of bedrock show significant variations in domain states from SD (in brown iron ore) to MD (for quartzite and gneiss) (Fig. 5 (d)). Indicators of the superparamagnetic grains demonstrate very low values: the relative FD% does not exceed 2.8% (in low-magnetic soils), with a mean value less than 1% (Fig. 5 (e)). Δ_{FD} values are also low (not shown), with maximal

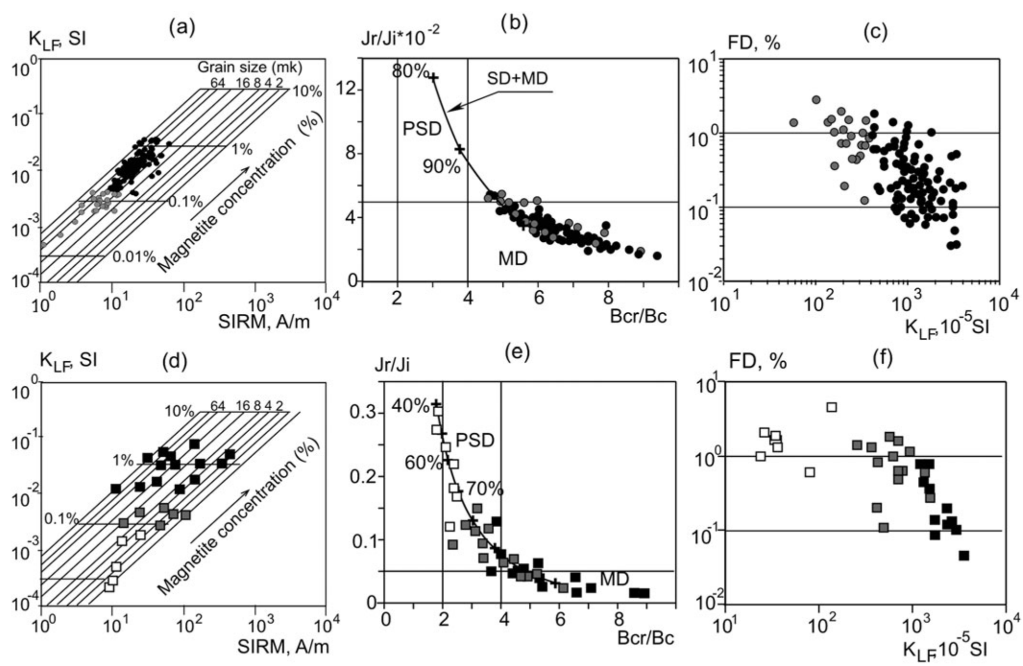

Figure 5 *Estimation of the effective size of the magnetic grains of soil (a) and bedrock (d); the domain state of the magnetic particles in soil (b) and bedrock (e); and indicators of the presence of superparamagnetic particles in soil FD% (c) and rock (f). Symbols as in Figure 3.*

values (14×10^{-5} to 18×10^{-5} units SI), which were found in samples of strongly magnetic soils. FD% values less than 1% are assumed to be insignificant, because they generally occur either in highly magnetic rocks or in soils with very low values of Δ_{FD}. These FD% values can be considered as zero.

We found no clear correlation between FD% and other magnetic parameters. SPM indicators demonstrate, first, the absence or very small concentrations of SP grains, which provide no influence on the overall magnetic properties of soil and rock, and, second, the irregularities of SP grain distribution in different types of rock and soil.

Bedrock shows implicit regularities in distribution of SPM particles: their noticeable concentration only occurs in brown iron ore (FD% increased up to 4.7%, Fig. 5 (e)). When brown iron ore is considered to be of authigenic origin, the presence of ultrafine particles (< 0.03 mm) is to be expected. In quartzite, gneiss and granite, there are practically no SPM grains; their relative FD% does not exceed 1%.

DISCUSSION

The magnetic susceptibility values measured in the Kurma archaeological region are quite different from those of other iron-smelting sites. In contrast to European iron-working centres with a low background of ground surface magnetic susceptibility (Powell *et al.* 2002; Vernon 2004; Powell 2008), the magnetic properties of the topsoil in Kurma are sufficiently enhanced due to enrichment by magnetite from the weathering products of the highly magnetic bedrock of Primorsky Ridge, which have been transported down slope. Even in the vicinity of smelting centres, located at the boundary between the areas of high and moderate values of magnetic susceptibility (areas A and B), the background topsoil K values are 10–15 times higher than those of the iron-working centres in Europe. A lesser magnetic contrast between the geological substrate and the components of the iron-smelting centre (bloomeries, slag blocks) results in a decrease of the magnetic survey resolution. The magnetic survey over the ‘Kurma Lake 1’ and ‘Kurma 28’ sites (Kharinsky and Snopkov 2004) has shown that magnetic anomalies over archaeological objects are caused by bloomeries, slag pits and connecting channels, while the other components of the iron-smelting complex, such as charcoal production pits and ore roasting areas, and places for grinding and storage of raw material did not appear in the magnetic field.

The topsoil in the charcoal roasting zone must be characterized by enhanced values of magnetic susceptibility (Powell 2008; Powell *et al.* 2012) and FD%. In the case of brown iron ore usage as raw material, the ore grinding (crushing) locales must be characterized by high coercivity (low values of the S-ratio and high values of B_c and B_{cr}). However, we have not observed such anomalies. If the absence of traces of charcoal production may be attributed to a large distance between the charcoal production and iron-smelting zones (up to 4 km from each other: Foard 2001), then the absence of ore preparation and storage areas, which must be located in the immediate vicinity of bloomeries, may be explained by an alternative type of raw material and/or different technologies of its preparation.

The question arises as to whether it is possible to consider the magnetite concentrate (black sand talus) from the soil surface layer as a potential source of raw material for ancient iron-smelting industry. Yes, several examples of such technology are known. Even Aristotle mentioned the use of enriched magnetic concentrate (magnetic sand) in the ancient iron-working industry (the so-called ‘halib’ and ‘amiss’ iron) (Kuparadze *et al*. 2009). Direct archaeological data attest that at the beginning of the first millennium BC, in the coastal area of western Georgia (Caucasus), a highly developed iron-working industry existed, using magnetic sands as raw material (Khakutaishvili 1973). The magnetic mineral composition of this sand (Gzelishvili 1964) is close to that of the black sand talus of Kurma.

An iron-smelting technology based on magnetite (titanomagnetite) sands is well studied at ancient African bloomery smelting sites. This technology involves the addition of quartz sand as a flux to lower the melting point of the gangue and extract more iron from the ore (van der Merwe and Killick 1979; Miller *et al.* 2001, Ige and Rehren 2002; Iles and Martinón-Torres 2009; Killick and Miller 2014). Such a process is possible with a TiO_2 content up to 20% in the initial raw material (Killick and Miller 2014). A relatively high content of titanium (up to 2%) and vanadium (up to 380 g ton^{-1}) in the Kurma slags confirms the application of this particular technology, because titanium and vanadium, found in slags and non-metallic inclusions of steel products, can result only from iron sand smelting (Cho *et al.* 2014).

Therefore, an iron-smelting industry based on magnetite sand was already known at the beginning of the Christian era and its technology is clear. Most probably, it had been used in the Kurma archaeological region. The development of such a smelting technology in Kurma was conditioned by several favourable circumstances, among them being: the high magnetite concentration of the initial sand; the lack of any necessity to grind the ore; and easy way to concentrate enrichment by washing; and convenient supply.

In East Asia, an iron sand smelting industry is known in Japan (since the sixth century AD) (Kitamura *et al.* 2002) and Korea (since the second century AD) (Park and Rehren 2011). Moreover, in the latter case, the developed iron sand smelting technology suggests cultural and technical relations with the north, most probably the Russian Maritime Province, as a source of knowledge (Park and Rehren 2011). Thus the discovery of an iron sand smelting industry at the Kurma site in the Baikal region raises the question of the distribution of technology and cultural relations in East Asia.

CONCLUSIONS

The analysis of the rock-magnetic properties of topsoil and bedrock from the study area and their spatial distribution allowed us to draw the following conclusions:

- In the vicinity of the iron-smelting centres of the Kurma archaeological region, the topsoil of the foothills and mountain slopes (areas A and B) shows very high magnetic susceptibility. The same and even higher magnetic susceptibility values are demonstrated by bedrock (granite gneiss, gneiss, ferruginous quartzite), exposed at altitudes of 800–1000 m within the study area. Highly magnetic rocks contain sufficient amounts (2–6%) of magnetic minerals, predominantly magnetite and Fe-rich titanomagnetite.
- The magnetic fraction of the soil mainly consists of multidomain grains of low-coercive magnetic minerals (magnetite and Fe-rich titanomagnetite) and coincides in composition with the magnetic fraction of the bedrock. The contribution of high-coercive minerals is negligibly low and does not affect the rock-magnetic properties of the rock as a whole. The brown iron ores mainly consist of iron hydroxide and paramagnetic minerals.
- The magnetic properties of the topsoil are defined only by their concentration of ferrimagnetic minerals. This means that the distribution of the rock-magnetic characteristics over the studied area is governed by the distance from the magnetic source and the peculiarities of the transport of magnetic material. Under the influence of gravitational sliding and slopewash, the weathered bedrock material is moved down slope and is deposited at its base. As a result, the highest magnetic characteristics are shown by soils near the outcrops of highly magnetic rocks on horizontal steps and at the feet of slopes, where the waterflows diminish. The

prevailing north-east winds in the Olkhon region result in wind dispersion of the magnetic material in a south-westerly direction.

- A high concentration of magnetite in the topsoil allows us to consider it to be magnetite sand, which could have been one of potential sources of ore concentrate for the iron-smelting process in the Kurma archaeological region, because it does not require large additional costs for the preparation of ores (crushing) and it can be used immediately after washing.
- The discovery of new type of iron-smelting industry at the Kurma site in the Baikal region based on iron sand gives us an opportunity to reconstruct the possible methods of distribution of technology and cultural relations in East Asia.

ACKNOWLEDGEMENTS

We would like to thank the two anonymous reviewers for their suggestions and comments. Following their suggestions, we included several improvements in the manuscript. The reported study was partially supported by the RFBR, research project No. 10-05-00263, 'Study the monuments of ancient iron metallurgy in Olkhon region by archaeogeophysical methods', and the RSF, research project No. 14-50-00036, 'Multidisciplinary research in archaeology and ethnography of North and Central Asia'.

REFERENCES

Abrahamsen, N., Jacobsen, B. H., Koppelt, U., Lasson, P., Smekalova, T., and Voss, O., 2003, Archaeomagnetic investigation of Iron Age slags in Denmark, *Archaeological Prospection*, **10**, 91–100.

Agafonov, Y. A., and Kozhevnikov, N. O., 1999, Geophysical survey in studying of archaeological site of Iron Age in Tchernorud locality (Olkhon region), in *Geophysics on the on the threshold of the third millennium, proceedings of the first workshop*, 215–224, IRTGU Publishing, Irkutsk (in Russian).

Batt, C., Fear, S., and Heron, C., 1995, The role of magnetic susceptibility as a geophysical survey technique: a site assessment at High Cayton, North Yorkshire, *Archaeological Prospection*, **2**, 179–196.

Birch, T., Scholger, R., Walach, G., Stremke, F., and Cech, B., 2015, Finding the invisible smelt: using experimental archaeology to critically evaluate fieldwork methods applied to bloomery iron production remains, *Archaeological and Anthropological Sciences*, **7**, 73–87.

Cho, Y., Cho, N., Han, J., and Rho, T., 2014, An experimental archaeological study on iron sand smelting in the Korean Peninsula, *ISIJ International*, **54**, 1038–1043.

Dalan, R. A., and Banerjee, S. K., 1998, Solving archaeological problems using techniques of soil magnetism, *Geoarchaeology*, **13**, 3–36.

Day, R., Fuller, M., and Schmidt, V. A., 1977, Hysteresis properties of titanomagnetites: grain-size and compositional dependence, *Physics of the Earth and Planetary Interiors*, **13**, 260–267.

Dunlop, D. J., 2002, Theory and application of the Day plot (M_{rs}/M_s versus H_{cr}/H_c), *Journal of Geophysical Research: Solid Earth*, **107**, 2046–2067.

Dunlop, D. J., and Özdemir, Ö., 1997, *Rock magnetism: fundamental and frontier*, Cambridge University Press, Cambridge.

Ellwood, B. B., Petruso, K. M., and Harrold, F. B., 1997, High-resolution paleoclimatic trends for the Holocene identified using magnetic susceptibility data from archaeological excavations in caves, *Journal of Archaeological Science*, **24**, 569–573.

Evans, M. E., and Heller, F., 2003, *Environmental magnetism: principles and applications of enviromagnetics*, Academic Press, Amsterdam.

Foard, G., 2001, Medieval woodland, agriculture and industry in Rockingham Forest, Northamptonshire, *Medieval Archaeology*, **45**, 41–95.

Gose, W. A., 2000, Palaeomagnetic studies of burned rocks, *Journal of Archaeological Science*, **27**, 409–421.

Gzelishvili, I. A., 1964, *Iron-smelting industry in ancient Georgia*, Mestniereba, Tbilisi (in Russian).

Herries, A. I. R., 2009, New approaches for integrating palaeomagnetic and mineral magnetic methods to answer archaeological and geological questions on Stone Age sites, in *New directions in archaeological science* (eds. A. Fairbairn,

S. O'Conner, and B. Marwick), 235–253, Terra Australis 28, Australian National University Press, Canberra, Australia.

Ige, A., and Rehren, T., 2002, Black sand and iron stone: iron smelting in Modakeke, *Ife, south western Nigeria, IAMS*, **22**, 19–21.

Iles, L., and Martinón-Torres, M., 2009, Pastoralist iron production on the Laikipia Plateau, Kenya: wider implications for archaeometallurgical studies, *Journal of Archaeological Science*, **36**, 2314–2326.

Jassonov, P. G., Nourgaliev, D. K., Bourov, B. V., and Heller, F., 1998, A modernized coercivity spectrometer, *Geologica Carpathica*, **49**, 224–226.

Kazansky, A. Y., Bezrukova, E. V., Krivonogov, S. K., Molodin, V. I., Matasova, G. G., Chemyakina, M. A., Abzaeva, A. A., Letunova, P. P., and Kulagina, N. V., 2007, A reconstruction of ancient men habitant environment for Lake Lozhka group of archaeological sites, in *Problems of archaeology, ethnography and anthropology of Siberia and adjacent territories: proceedings of annual session* (eds. A. P. Derevianko and V. I. Molodin), 249–254, Vol. **13**, IAE SO RAN Publishing, Novosibirsk (in Russian).

Khakutaishvili, D. A., 1973, On the history of ancient Kolkhida iron smelting: questions of ancient history, *Caucasus and the Middle East Bulletin*, **4**, 170–179. (in Russian).

Kharinsky, A. V., and Snopkov, A. V., 2004, Iron production by population of Olkhon region in Elga time, in *Proceedings of the Laboratory of Ancient Technologies*, 167–187, Vol. **2**, Irkutsk (in Russian).

Killick, D., and Miller, D., 2014, Smelting of magnetite and magnetite–ilmenite iron ores in the northern Lowveld, South Africa, ca. 1000 CE to ca. 1880 CE, *Journal of Archaeological Science*, **43**, 239–255.

Kitamura, T., Katayama, H., Anazawa, Y., Haba, M., Kishida, N., and Murakawa, Y., 2002, Control of slag and inclusions in traditional Japanese iron- and steelmaking, *Ironmaking and Steelmaking*, **29**, 276–280.

Kochnev, A. P., 2007, *Olkhon crystalline complex: problems of geology and mineralogy of Olkhon region*, IRTGU Publishing, Irkutsk (in Russian).

Kozhevnikov, N. O., Kharinsky, A. V., and Kozhevnikov, O. K., 2001, An accidental geophysical discovery of an Iron Age archaeological site on the western shore of Lake Baikal, *Journal of Applied Geophysics*, **47**, 107–122.

Kozhevnikov, N. O., Kozhevnikov, O. K., and Kharinsky, A. V., 1998, How the search for a solution of geophysical problems have led to the discovery of archaeological site, *Geofizika*, **6**, 48–60. (in Russian).

Kuparadze, D. M., Pataridze, D. V., and Kerestedjian, T. N., 2009, Ancient Georgian iron metallurgy and its ore base, in *Geoarchaeology and archaeomineralogy: proceedings of the international conference (Sofia, 2008)* (eds. R. I. Kostov, B. Gaydarska, and M. Gurova), 248–252, Publishing House 'St. Ivan Rilski', Sofia.

Liu, Q., Deng, C., Yu, Y., Torrent, J., Jackson, M. J., Banerjee, S. K., and Zhu, R., 2005, Temperature dependence of magnetic susceptibility in an argon environment: implications for pedogenesis of Chinese loess/palaeosols, *Geophysical Journal International*, **161**, 102–112.

Mighall, T. M., Foster, I. D. L., Crew, P., Chapman, A. S., and Finn, A., 2009, Using mineral magnetism to characterize ironworking and to detect its evidence in peat bogs, *Journal of Archaeological Science*, **36**, 130–139.

Miller, D., Killick, D., and van der Merwe, N., 2001, Metalworking in the northern Lowveld, South Africa, AD 1000–1890, *Journal of Field Archaeology*, **28**, 401–417.

Morinaga, H., Inokuchi, H., Yamashita, H., Ono, A., and Inada, T., 1999, Magnetic detection of heated soils at Palaeolithic sites in Japan, *Geoarchaeology*, **14**, 377–399.

Park, J.-S., and Rehren, T., 2011, Large-scale 2nd to 3rd century AD bloomery iron smelting in Korea, *Journal of Archaeological Science*, **38**, 1180–1190.

Peters, C., Church, M. J., and Mitchell, C., 2001, Investigation of fire ash residues using mineral magnetism, *Archaeological Prospection*, **8**, 227–237.

Peters, C., Abrahamsen, N., Voss, O., Batt, C. M., and McDonnel, G., 2008, Magnetic investigations of Iron Age slags at Yderik, Denmark: mineral magnetic comparison to UK slags, *Physics and Chemistry of the Earth*, **33**, 465–473.

Powell, A. J., 2008, *The magnetic signatures of medieval and post-medieval pyrotechnical industries*, Ph.D. thesis, University of Bradford.

Powell, A. J., Wheeler, J., and Batt, C. M., 2012, Identifying archaeological wood stack charcoal production sites using geophysical prospection: magnetic characteristics from a modern wood stack charcoal burn site, *Journal of Archaeological Science*, **39**, 1197–1204.

Powell, A. J., McDonnell, J. G., Batt, C. M., and Vernon, R. W., 2002, An assessment of the magnetic response of an iron-smelting site, *Archaeometry*, **44**, 651–665.

Ryazanov, G. V., 1993, *Geological monuments of Baikal*, Nauka, Novosibirsk (in Russian).

Shulga, V. V., 2010, *Migmatites of Olkhon crystalline complex and their mineragenic significance*, Ph.D. thesis, University of Irkutsk (in Russian).

Snpokov, S. V., Matasova, G. G., Kazansky, A. Y., Kharinsky, A. V., and Kozhevnikov, N. O., 2012, Ore sources for iron smelting in ancient times: Kurma archaeological region, in *Proceedings of the Laboratory of Ancient Technologies*, 10–30, Vol. **9**, Irkutsk (in Russian).

Thompson, R., and Oldfield, F., 1986, *Environmental magnetism*, George Allen & Unwin, London.

Ufimtsev, G. F., 1995, *Geomorphology practice in Transbaikalia*, Irkutsk (in Russian).

van der Merwe, N. J., and Killick, D. J., 1979, Square: an iron smelting site near Phalaborwa, *South African Archaeological Society, Goodwin Series*, **3**, 86–93.

Vernon, R. W., 2004, *Application of archaeological geophysical techniques to the investigation of British smelting sites*, Ph.D. thesis, University of Bradford.

Vernon, R. W., McDonnell, J. G., and Schmidt, A., 1998, An integrated geophysical and analytical appraisal of early iron working: three case studies, *Historical Metallurgy*, **32**, 67–81.

Vigliotti, L., Roveri, M., and Capotondi, L., 2003, Etruscan archaeometallurgy record in sediments from the northern Tyrrhenian Sea, *Journal of Archaeological Science*, **30**, 809–815.